Synthesis of Schiff base-ester linked 6-bromobenothiazole based novel liquid crystalline compounds

Sejal B. Patel
Department of Chemistry
C.B.Patel omputer & J.N.M Patel Science College,
Bharthana (Vesu), Surat, Gujarat, India.
Email:- seju1296@gmail.com

Nilesh G. Limbachiya
Department of Chemistry
C.B.Patel omputer & J.N.M Patel Science College,
Bharthana (Vesu), Surat, Gujarat, India.
Email:- n.g.limbachiya@gmail.com

Abstract:

Two different types of homologues series with a Schiff-base ester central linkage involving 2-amino-6-bromobenzothiaole moiety based liquid crystals, namely 4-(1-((6-bromobenzo[d] thiazol-2-yl)imino)ethyl)phenyl 4-(Alkoxy)benzoate (Series-I) and 4-(1-((6-bromobenzo[d]thiazol-2-yl)imino)ethyl)-3-hydroxyphenyl 4-(Alkoxy)benzoate (Series-II) were synthesized and their mesophase characteristics and thermal behavior were evaluated. Differential scanning calorimetry (DSC) was used to study mesophase transitions, and polarized optical microscopy (POM) was carried out to identify the mesophase. The results show that all compounds of both series exhibit enantiotropic nematic phase. In Series-I, C7 to C14 derivatives exhibit Smectic A (SmA) phase. Whereas, in Series-II Smectic A phase showed from C6 derivative and persist up to last member of the series. The thermal stability od Series-II is higher than that of Series-I because of the introduction of lateral hydroxyl group (-OH), which enhanced intermolecular hydrogen bonding, molecular polarity, dipole-dipole interactions and lateral cohesion among molecules.

Introduction:

Since the pioneering observation of liquid crystalline behaviour by Friedrich Reinitzer, considerable research has been devoted to developing molecular structures that exhibit desirable liquid-crystalline characteristics over broad temperature ranges. A major objective in this field is to establish a clear structure–property relationship between the molecular architecture of a mesogen and its resulting physical and mesomorphic properties. Understanding this relationship is particularly important for the systematic design of liquid crystalline materials for electro-optical and other advanced technological applications [1–4]. In addition to their technological significance, liquid crystalline materials have attracted attention in pharmaceutical and biomedical fields because of their ability to improve stability, hydration, and controlled-release characteristics, making them promising candidates for drug-delivery applications [5]. Their well-defined molecular organization and responsive properties have also encouraged their investigation as functional nanomaterials for advanced electro-optical devices [6].

Liquid crystals can broadly be classified into thermotropic and lyotropic systems according to the conditions under which their mesophases are generated [7,8]. The mesomorphic behaviour of a liquid crystalline compound is strongly governed by its molecular structure and several associated structural parameters. Important factors include molecular geometry, the nature and orientation of connecting groups [9], the number and arrangement of aromatic or heterocyclic rings [10], the length of terminal alkyl or alkoxy chains [11], and the

electronic and steric characteristics of terminal substituents [12]. Furthermore, intermolecular interactions play a crucial role in determining molecular organization and consequently influence the formation, stability, and temperature range of different mesophases [13]. These structural features collectively contribute to the development of an appropriate balance between molecular rigidity and flexibility, which is essential for the formation of calamitic liquid crystalline architectures [14]. Schiff bases constitute an important class of organic compounds characterized by the presence of an imine functional group. They are generally synthesized through a condensation reaction between an aldehyde or ketone and a primary amine, accompanied by the elimination of water. Depending on the precursor molecules, the resulting compounds contain an imine linkage such as –CH=N– or –C=N–. Schiff base derivatives have attracted extensive scientific interest because of their diverse chemical and functional properties, including their applications as stabilizing agents, ligands and chelating agents, biologically active compounds, and materials for photoconductive applications. The imine linkage is also of considerable importance in liquid crystal chemistry because it provides an effective structural unit for constructing rigid and conjugated mesogenic systems. Numerous studies have demonstrated that incorporation of Schiff base functionality can significantly influence molecular organization and promote the development of liquid crystalline mesophases [15–31].

Lateral substitution is another important structural factor that can significantly influence the packing efficiency of mesogenic molecules. A substituent introduced at a lateral position relative to the principal molecular axis can disturb the regular arrangement of the rigid core and consequently modify the stability of the liquid crystalline phase. Although such steric disruption may reduce the efficiency of molecular packing, it can also be beneficial because it provides an opportunity to tune the physical and mesomorphic characteristics of the material. Consequently, lateral substitution can be deliberately employed to obtain specific properties that are desirable for particular technological applications [32-35]. The size of a lateral substituent is particularly important in determining the thermal behaviour of a mesogen. An increase in the steric bulk of the substituent attached to the rigid molecular core generally produces a decrease in the nematic-to-isotropic (N–I) transition temperature. This tendency can occur even when the substituent possesses favourable electronic characteristics, such as appreciable polarity or polarizability, because steric effects and disruption of molecular packing can become dominant factors. Therefore, relatively small lateral substituents are generally more effective in preserving the ordered molecular arrangement and maintaining

liquid crystalline behaviour, whereas bulky lateral groups may substantially disturb the packing of the mesogenic core [36,37]

Characterization:

Elemental analysis (C, H, N) was performed using a PerkinElmer 2400 Series II CHN analyzer (USA) at SAIC, Tezpur University, Assam. Infrared spectra were recorded using a PerkinElmer Spectrum BXw spectrophotometer at the Centre of Excellence, Vapi, in the frequency range 4000–400 cm−1 with samples embedded in KBr discs. High resolution (400 MHz) NMR Spectra of the mesogenic compounds were recorded using Bruker Avance 400 MHz spectrometer (Bruker TopSpin software) at the Gandhigram rural university, Tamilnadu. Thin-layer chromatography (TLC) analyses were performed using aluminium-backed silica-gel plates (Merck60 F524) and examined under shortwave UV light. Thermal (DSC) analyses of the liquid crystalline compounds were carried out by Centre of Exellence, Vapi. DSC analyses were performed on a Mettler M-3 thermo balance (Switzerland) with microprocessor TA-300 instrument at a heating rate of 10◦C/min in a N2 atmosphere. The optical microscopy studies were determined by using polarizing microscope Nikon Eclipse 50i POL equipped with Linkam Analysa-LTS420 hot stage, using a standard procedure in our department.

Materials:

All chemicals required for the synthesis of the homologous series were procured from standard industrial sources and used with appropriate purification when necessary. 4-Hydroxybenzoic acid, alkyl bromides, N,N′-dicyclohexylcarbodiimide (DCC), and 4-dimethylaminopyridine (DMAP) were obtained from Chemdyes. Solvents such as dichloromethane (DCM), along with 4-bromoaniline, were supplied by A R Scientific (Navsari). Other reagents including Bromine, Potassium Thiocyanate, Acetone, Ethanol, Methanol, Acetic acid, Hydrochloric acid, Potassium Hydroxide, Sodium Hydroxide and Ammonium Hydroxide were used as received unless stated otherwise. All solvents were purified following standard laboratory procedures prior to use.

Synthesis:

Synthesis of 2-Amino-6-bromobenzothiazole

2-Amino-6-bromobenzothiazole was synthesized from 4-nitroaniline following the reported procedure [38]. A solution containing p-bromoaniline (5 mmol) and potassium thiocyanate (3.04 g, 20 mmol) in 98% acetic acid (18 mL) was prepared. Subsequently, a bromine solution (0.8 g, 5 mmol) in acetic acid (4 mL) was added slowly while maintaining the reaction temperature below 35°C. After complete addition of bromine, the reaction mixture was stirred continuously for 10 h. Upon completion of the reaction, the precipitated product

was filtered and washed thoroughly with water. The filtrate was then neutralized using ammonium hydroxide, resulting in the formation of the desired compound. The obtained solid was filtered and recrystallized from aqueous ethanol (1:1) to yield pure pale-yellow needle-shaped crystals of 2-amino-6-nitrobenzothiazole. Yield: 87% Melting point: 184°C

Synthesis of 4'-n-alkoxy benzoic acid

Several methods have been reported in the literature for the alkylation of 4-hydroxy benzoic acid [39-42]. In the present investigation, the procedure developed by Dave and Vora [43] was adopted. A mixture of 4-hydroxy benzoic acid (13.8 g, 0.1 mol), the corresponding n-alkyl bromide (23.20 mL, 0.12 mol), and potassium hydroxide (14.0 g, 0.25 mol) was dissolved in methanol/ethanol (100 mL) in a round-bottom flask equipped with a reflux condenser. The reaction mixture was refluxed on a water bath for about 8–10 h. Subsequently, 10% aqueous KOH solution (25 mL) was added, and refluxing was continued for an additional 2–3 h to hydrolyze any ester formed during the reaction. After cooling to room temperature, the reaction mixture was acidified by pouring it into an ice-cold dilute HCl-water mixture (1:1). The precipitated product was filtered, washed with water, and dried under vacuum. The resulting alkoxy benzoic acids were recrystallized repeatedly from methanol until constant transition temperatures were obtained. The observed transition temperatures were found to be in close agreement with the literature values.

Synthesis of 4-acetylphenyl 4-alkoxybenzoate

The intermediates were synthesized through esterification between appropriate 4-hydroxyacetophenone and 4′-n-alkoxy benzoic acid. Equimolar quantities of 4-hydroxyacetophenone (2.22 mmol) and the corresponding 4′-n-alkoxy benzoic acid (2.22 mmol) were dissolved in dry dichloromethane (20 mL). To this solution, N,N′-dicyclohexylcarbodiimide (DCC) (2.22 mmol) and a catalytic amount of dimethylaminopyridine (DMAP) were added. The reaction mixture was stirred at room temperature overnight. During the reaction, a white precipitate formed, which was removed by Buchner filtration. The filtrate was concentrated under reduced pressure to obtain the crude product. Purification was carried out using silica gel column chromatography with dichloromethane as the eluent, followed by repeated recrystallization from ethanol until constant transition temperatures were achieved.

Synthesis of 4-(1-((6-bromobenzo[d]thiazol-2-yl)imino)ethyl)phenyl 4-(Alkoxy) benzoate (Series--I)

A mixture of 4-acetylphenyl 4-alkoxy benzoate (0.01 mol) and 2-amino-6-bromobenzothiazole (0.01 mol) was dissolved in absolute ethanol (10 mL). To this mixture, 2–3 drops of acetic acid were added as a catalyst, and the reaction mixture was refluxed for 3–4 h. After refluxing, the mixture was allowed to cool and further stirred overnight at room temperature. The solvent was removed under reduced pressure to obtain the crude residue, which was then purified by silica gel column chromatography (100–200 mesh) using petroleum ether (60–80°C) and ethyl acetate (7:3) as the eluent system. Evaporation of the solvent afforded the solid product, which was repeatedly recrystallized from ethanol until constant transition temperatures were obtained. The purity of the synthesized compounds was confirmed by thin-layer chromatography using Merck Kieselgel 60 F254 precoated plates.

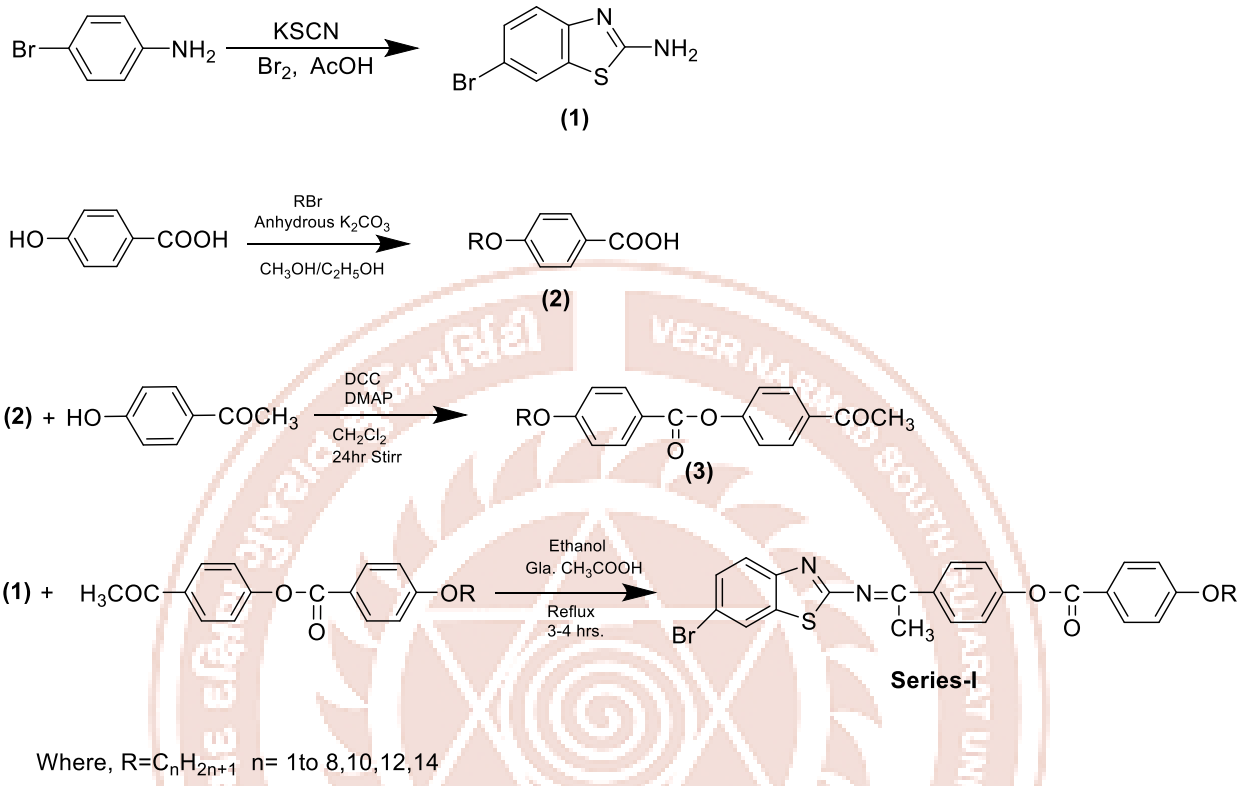
Synthesis of 4-acetyl-3-hydroxyphenyl 4-alkoxybenzoate

The intermediate compounds were synthesized through an esterification reaction between the corresponding 4′-n-alkoxy benzoic acid and 2,4-dihydroxyacetophenone. Equimolar amounts of 4′-n-alkoxy benzoic acid and 2,4-dihydroxyacetophenone (2.22 mmol each) were dissolved in dry dichloromethane (20 mL). To this reaction mixture, dicyclohexylcarbodiimide (DCC) (2.22 mmol) and dimethylaminopyridine (DMAP) (0.2 mmol) were added, and the mixture was stirred overnight at room temperature. During the course of the reaction, a white precipitate of dicyclohexylurea was formed, which was removed by Buchner filtration. The filtrate was then concentrated under reduced pressure to obtain the crude product. Purification was carried out by silica gel column chromatography using dichloromethane as the eluent, followed by repeated recrystallization from ethanol until constant transition temperatures were achieved.

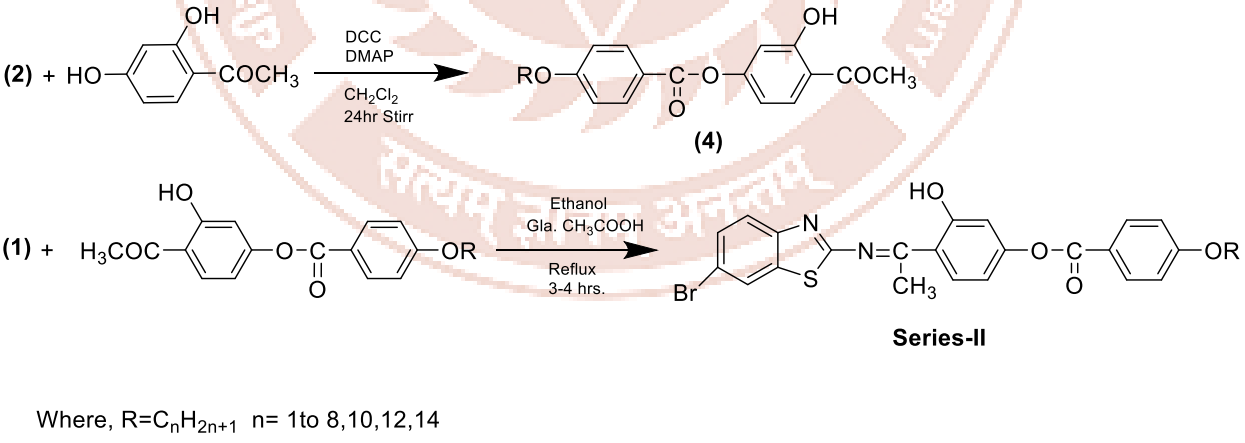
Synthesis of 3-hydroxy-4-(1-((6-bromobenzo[d]thiazol-2-yl)imino)ethyl)phenyl 4-(Alkoxy)benzoate (Series-II)

A mixture of 4-acetyl-3-hydroxyphenyl 4-alkoxybenzoate (0.01 mol) and 2-amino-6-bromobenzothiazole (0.01 mol) was dissolved in ethanol (10 mL). The reaction mixture was refluxed for 3–4 h in the presence of 2–3 drops of acetic acid, which acted as a catalyst. After completion of refluxing, the mixture was allowed to cool and subsequently stirred overnight at room temperature. The reaction mixture was filtered, and the filtrate was kept in a fume hood to allow slow evaporation of the solvent at room temperature. The obtained residue was purified by silica gel column chromatography (100–200 mesh) using a petroleum ether (60–80°C) and ethyl acetate mixture (7:3) as the eluent system. Evaporation of the solvent from the

collected fractions afforded the desired solid product. The compound was further purified by repeated recrystallization from ethanol until constant transition temperatures were obtained. The purity of the synthesized compounds was confirmed by thin-layer chromatography using Merck Kieselgel 60 F254 precoated plates.



Scheme:1 Synthetic route of Series-I



Scheme:2 Synthetic route of Series-II

Result and Discussion:

Spectral Data:

***4-(1-((6-bromobenzo[d]thiazol-2-yl)imino)ethyl)phenyl 4-(pentyloxy) benzoate* (BS$_5$)**

Molecular formula: $C_{27}H_{25}BrN_2O_3S$; Yield: 79%; UV-Vis ($CHCl_3$) λmax: 228nm, 469 nm; Elemental analysis data: Found; C: 60.37%, H: 4.70%, N: 5.12%, Calculated;

C: 60.33%, H: 4.68%, N: 5.21%; FT-IR (KBr): υ_{max}/cm^{-1} 3092 cm^{-1} (C-H str. aromatic), 2952, 2858 cm^{-1} (C-H str. aliphatic), 1729 cm^{-1} (C=O str. ester linkage), 1626 cm^{-1} (CH=N str. azomethine linkage), 1512 cm^{-1} (C=C str. aromatic ring), 1056 cm^{-1} (C-S-C). ^{1}H NMR (400 MHz DMSO): δ/ppm 0.92 (t, CH_3), 1.32-1.78 (m, CH_2), 2.52 (t, CH_3 azomethine), 3.16-4.09 (t, OCH_2), 7.10-8.10 (m, Ar-H). ^{13}C NMR (DMSO): δ/ppm 14.34 ($\underline{C}H_3$), 22.35-33.82 ($\underline{C}H_2$), 68.47 ($O\underline{C}H_2$), 112.54-163.84 (Ar-$\underline{C}$), 164.25 ($\underline{C}H$=N), 167.63 ($\underline{C}$=O). MS ES+ m/z (rel.int%): 538.8 (M+1) m/z.

3-hydroxy-4-(1-((6-bromobenzo[d]thiazol-2-yl)imino)ethyl)phenyl 4-(pentyloxy) benzoate (BD5)

Molecular formula: $C_{27}H_{25}BrN_2O_4S$; Yield: 77%; UV-Vis ($CHCl_3$) λmax: 222 nm, 369 nm; Elemental analysis data: Found; C: 58.67%, H: 4.87%, N: 5.61%, Calculated; C: 58.58%, H: 4.55%, N: 5.06%; FT-IR (KBr): υ_{max}/cm^{-1} 3078 cm^{-1} (C-H str.aromatic), 2933, 2726 cm^{-1} (C-H str. aliphatic), 1680 cm^{-1} (C=O str. ester linkage), 1632, 1589 cm^{-1} (CH=N str. azomethine linkage), 1527-1490 cm^{-1} (C=C str. aromatic ring), 1051 cm^{-1} (C-S-C), 3450 cm^{-1} (-OH str.) ^{1}H NMR (400 MHz DMSO): δ/ppm 0.86-0.87 (t, CH_3), 1.26-1.91 (m, CH_2), 4.05-4.08 (t, OCH_2), 6.88-8.07 (m, Ar-H), 2.51-2.65 (t, CH_3 azomethine linkage), 12.22 (s, OH). ^{13}C NMR (DMSO): δ/ppm 14.41 ($\underline{C}H_3$), 22.57-29.20 ($\underline{C}H_2$), 68.48 ($O\underline{C}H_2$), 111.10-162.60 (Ar-$\underline{C}$), 163.92 ($\underline{C}$=N azomethine linkage), 167.61 ($\underline{C}$=O). MS ES+ m/z(rel.int%): 551.8 (M-2) m/z.

3-hydroxy-4-(1-((6-bromobenzo[d]thiazol-2-yl)imino)ethyl)phenyl 4-(dodecyloxy)benzoate (BD12)

Molecular formula: $C_{34}N_{39}BrN_2O_4S$, Yield: 79%, UV-Vis ($CHCl_3$) λmax: 222 nm, 367 nm; Elemental analysis data: Found; C: 62.69%, H: 6.42%, N: 4.28%, Calculated; C: 62.66%, H: 6.03%, N: 4.29%; FT-IR (KBr): υ_{max}/cm^{-1} 3119 cm^{-1} (C-H str. aromatic), 2925, 2853 cm^{-1} (C-H str. aliphatic), 1730 cm^{-1} (C=O str. ester linkage). 1637, 1606 cm^{-1} (CH=N str. azomethine linkage), 1530-1510 cm^{-1} (C=C str. aromatic ring), 1074 cm^{-1} (C-S-C), 3445 cm^{-1} (-OH str.) ^{1}H NMR (400MHz DMSO): δ/ppm 0.87-0.88 (t, CH_3), 1.28-1.77 (m,CH_2), 4.06-4.09 (t, OCH_2), 6.87-8.07 (m, Ar-H), 2.50-2.65 (t, CH_3 azomethine linkage), 12.22 (s, OH). ^{13}C NMR (DMSO): δ/ppm 14.40 ($\underline{C}H_3$), 22.52-28.96 ($\underline{C}H_2$) 68.49 ($O\underline{C}H_2$), 111.11-162.60 (Ar-$\underline{C}$), 163.87 ($\underline{C}$=N azomethine linkage), 168.49 ($\underline{C}$=O). MS ES+ m/z(rel.int%): 654.6 (M+3) m/z.

Table:1 Transition temperature data of Series-I

Compound No.	R=C_nH_{2n+1} n=	Cr		SmA		N		I
BS_1	1	•	152	•	-	•	197	•
BS_2	2	•	145	•	-	•	194	•
BS_3	3	•	147	•	-	•	186	•
BS_4	4	•	139	•	-	•	183	•
BS_5	5	•	133	•	-	•	177	•
BS_6	6	•	126	•	-	•	167	•
BS_7	7	•	121	•	130	•	159	•
BS_8	8	•	115	•	127	•	154	•
BS_{10}	10	•	108	•	124	•	150	•
BS_{12}	12	•	97	•	116	•	145	•
BS_{14}	14	•	90	•	115	•	137	•

Table:2 Transition temperature data of Series-II

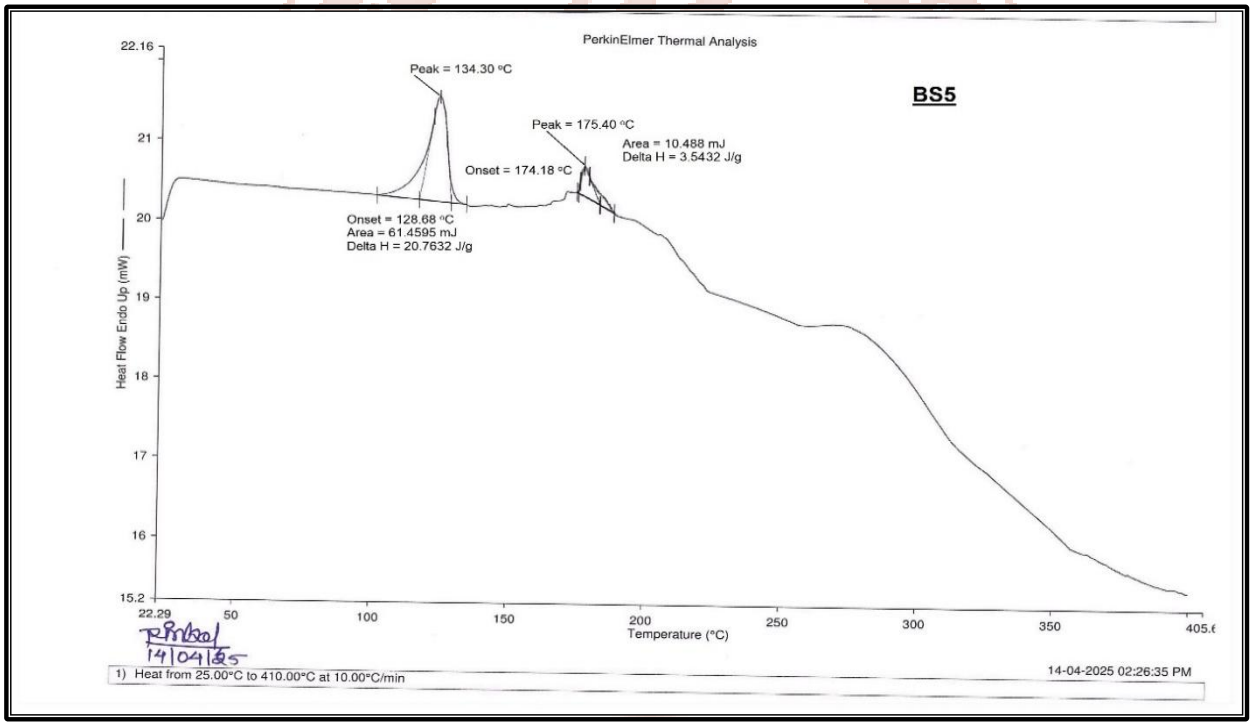
Compound No.	R=C_nH_{2n+1} n=	Cr		SmA		N		I
BD_1	1	•	169	•	-	•	215	•
BD_2	2	•	163	•	-	•	209	•
BD_3	3	•	171	•	-	•	206	•
BD_4	4	•	157	•	-	•	198	•
BD_5	5	•	149	•	-	•	190	•
BD_6	6	•	134	•	145	•	185	•
BD_7	7	•	128	•	143	•	178	•
BD_8	8	•	121	•	135	•	173	•
BD_{10}	10	•	124	•	137	•	168	•
BD_{12}	12	•	105	•	136	•	162	•
BD_{14}	14	•	99	•	127	•	156	•

Table:3 DSC data of the Series-I and II

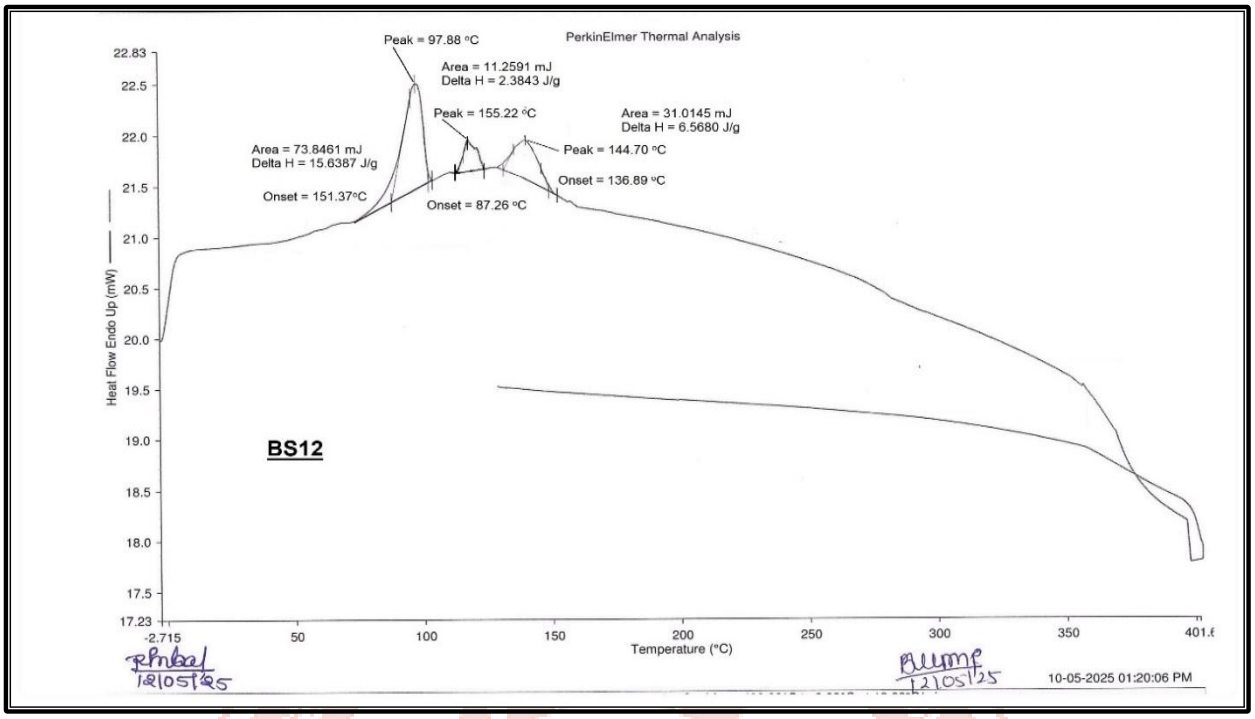
Series	Compound No	Transition	Peak/(POM) Temp. ^oC	ΔH J/g	ΔS $Jg^{-1}K^{-1}$
V	BS_5	Cr-N	134.30 (133)	20.7632	0.050959
		N-I	175.40 (177)	3.5432	0.007899

	BS_{12}	Cr-SmA	97.88 (97)	15.6387	0.042149
		SmA-N	115.22 (116)	2.3843	0.006139
		N-I	144.70 (145)	6.568	0.015719
VI	BD_5	Cr-N	150.18 (149)	17.1656	0.040549
		N-I	190.59 (190)	5.5387	0.011944
	BD_{12}	Cr-SmA	103.75 (105)	16.62	0.044097
		SmA-N	134.85 (136)	3.0159	0.007392
		N-I	164.78 (162)	4.899	0.011187

Figure 1 (a, b): DSC thermogram of Series-I

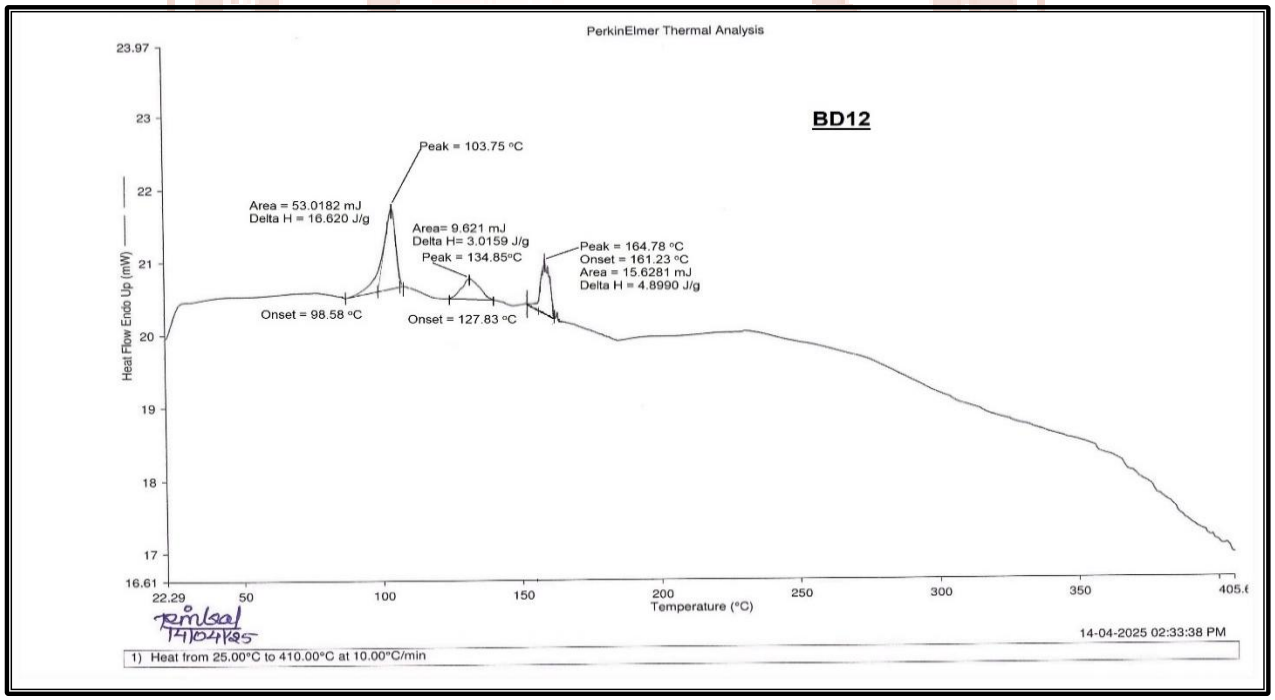


(a)

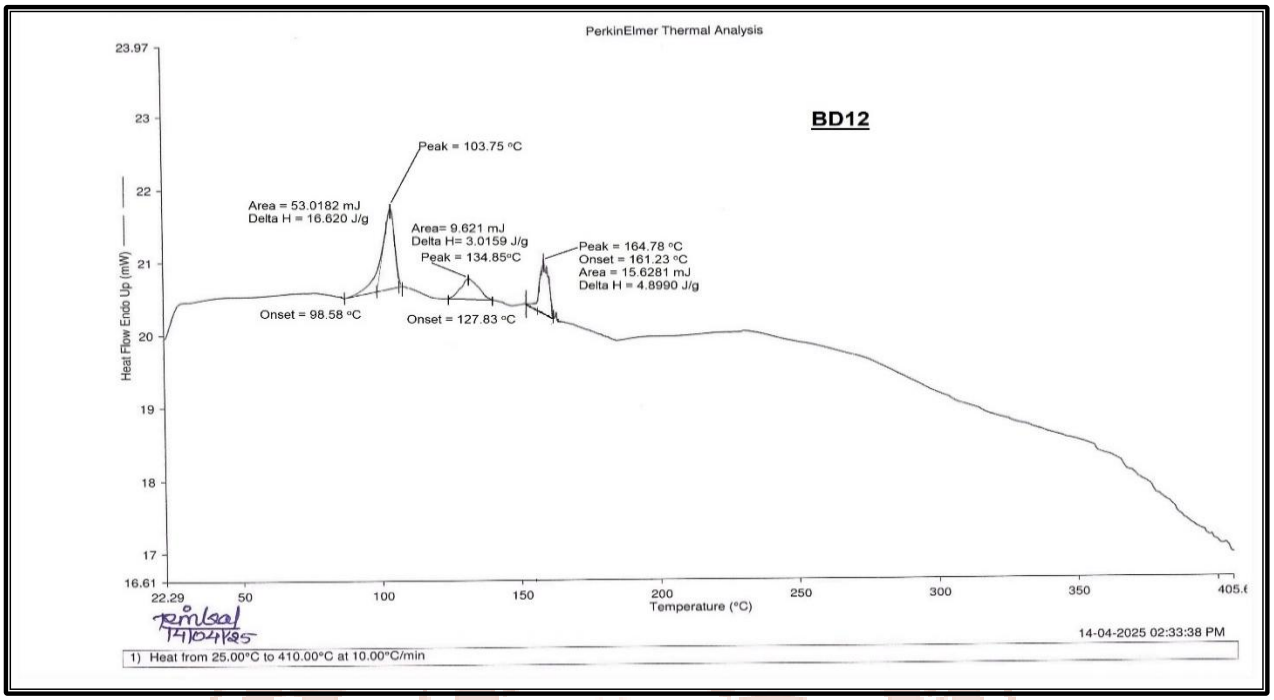


(b)

Figure 2 (a, b): DSC thermogram of Series-II



(a)



(b)

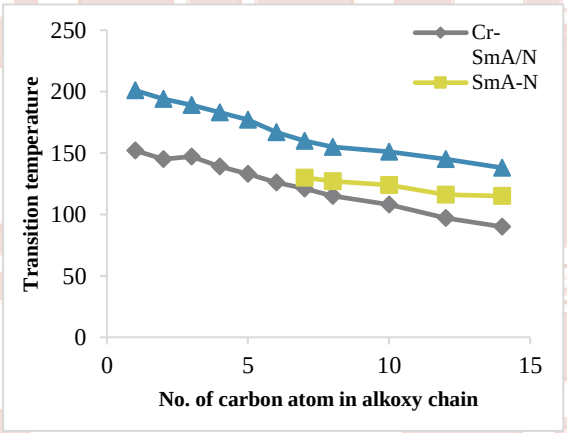


Figure 3: Transition temperature curve of Series-I

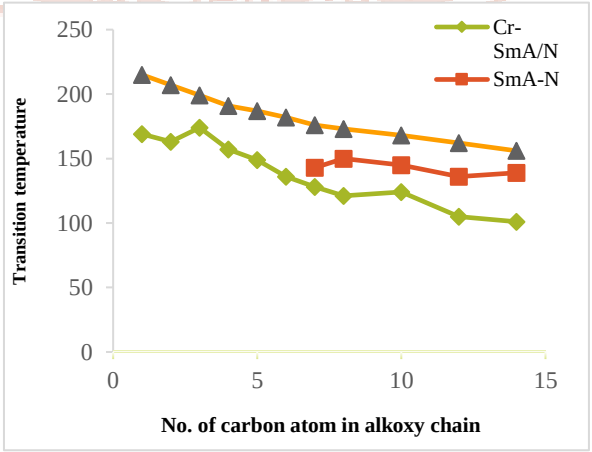


Figure 4: Transition temperature curve of Series-II

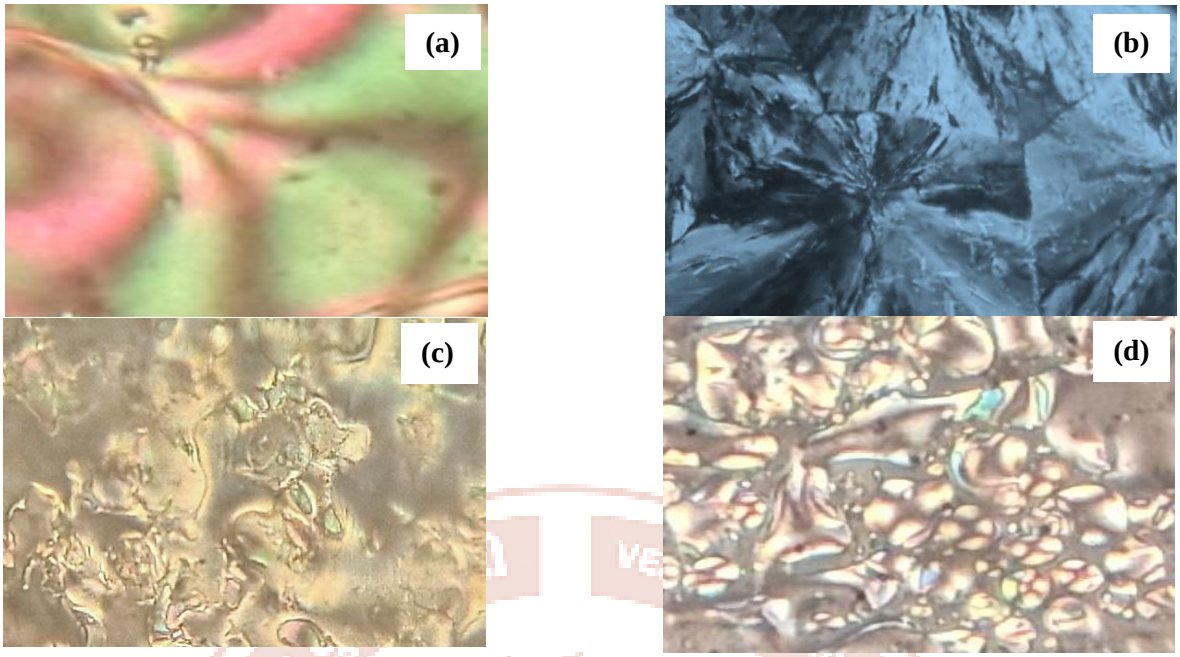


Figure 5: Optical micro photograph observed under POM: (a) Nematic phase at 133 ^{o}C (BS_5), (b) Smectic phase at 97 ^{o}C (BS_{12}), (c) Nematic texture at 149 ^{o}C (BD_5), (d) Smectic texture at 105 ^{o}C (BD_{12}).

Mesomorphic behavior:

The thermal transition temperatures and mesomorphic behavior of all the synthesized compounds were observed using a polarizing optical microscope (POM) and differential scanning calorimetry (DSC).

The thermal and mesomorphic behavior of Series-I compounds was studied as a function of the terminal alkoxy chain length and the corresponding transition temperature data are presented in Table 1, while the graphical representation is shown in Figure 3. Table 1 indicated that the lower homologues from C1 to C6 (methoxy to hexyloxy) derivatives exhibit A simple Cr-N-I phase sequence, indicating the presence of nematic mesophase. From the C7 homologue onward, the phase sequence changes to Cr-SmA-N-I, indicating the appearance of a smectic A phase in the higher homologues. Figure 3 illustrate that increasing alkoxy chain length favours the formation and stabilization of the SmA phase, while nematic phase becomes comparatively less dominant. The small irregularities in the curves may be associated with differences in molecular packing and the odd-even effect of the alkoxy chain.

Series-II shows similar chain-length-dependent trend but exhibits significant differences because of the presence of the presence of the lateral ortho-hydroxyl (-OH) group. From Table 2, C1-C5 homologues display Cr-N-I phase sequence, whereas the SmA phase appears from the C6 homologue and persists up to C14 homologue. Figure 4 shows the graph of transition temperature versus the number of carbons in alkoxy chain, which indicated that

all the transition temperatures decreases with increasing alkoxy chain length, although a small odd-even effect observed in Cr-N phase transition temperature.

DSC serves as an essential analytical tool for identifying thermal phase transitions in liquid crystalline materials. It provides quantitative information that facilitates the understanding of the phase behavior occurring during thermal transitions. The phase transition temperatures, together with the corresponding enthalpy changes (ΔH), of compounds BS5, BS12, BD5 and BD12 were determined using DSC analysis. The experimental results are presented in Table 3, which further confirm the mesophases identified through polarizing optical microscopy (POM). In addition to the transition temperatures, Table 3 also lists the enthalpy (ΔH) and molar entropy (ΔS) values for selected compounds from Series-I (BS5 and BS12) and Series-II (BD5 and BD12). Representative DSC thermograms of these compounds are illustrated in Figures 1 (a, b) and 2 (a, b). The transition temperatures obtained from microscopic observations were found to be in close agreement with DSC results, thereby confirming the reliability of the thermal analysis and the mesophase assignments.

In Series-II, the molecular structure is similar to Series-I but contains an additional lateral ortho hydroxyl (-OH) group on the central phenyl ring. This structural modification significantly influences the mesomorphic properties. The hydroxyl group increases molecular polarity and can participate in intermolecular hydrogen bonding, thereby strengthening the cohesive interactions between neighboring molecules. Consequently, Series-II generally exhibit higher transition temperatures than corresponding Series-I compounds.

Texture Study:

The optical microscopy studies were carried out with a “NICON ECLIPSE 50i POL” (Japan) equipped with Linkam Analysa-LTS 420 hot stage. The textures of the compounds were observed using polarized light with crossed polarizers with sample in thin film sandwiched between a glass slide and cover slip. The textures of compounds of Series-I and II are shown in Figure 5. Compound BS5 shows nematic texture on heating the solid at 133 oC. Compound BS12 shows smectic texture at 97 oC. In Series-IV Compound BD5 shows nematic phase at 149 oC and BD12 smectic phase at 105 oC..

Conclusion:

In this study, two new series of Schiff base-ester derivatives were synthesized and characterized with FT-IR, ^{1}H-NMR, ^{13}C-NMR and C, H, N technique, the relationship between the structure and their mesomorphic behavior were studied and tested by using POM and DSC. All the derivatives of Series-I and II show liquid crystalline behavior. The comparison of Series-I and II clearly demonstrates that the lateral hydroxyl (-OH) group in Series-II promotes smectic ordering. the smectic

phase appears from C_6 homologue, whereas in Series-I it appears from C_7 homologue. This earlier appearance indicates that hydrogen bonding and increased polarity associated with the hydroxyl group favour a more ordered layered arrangement. The longer alkoxy chains further enhance this tendency by increasing the flexible-chain contribution and promoting segregation of rigid aromatic and flexible aliphatic regions. Therefore, the combined presence of the lateral hydroxyl (-OH) group and longer alkoxy chain is particularly favourable for SmA formation and stabilization. The comparison also indicates that Series-II exhibits superior mesomorphic properties and thermal stability compared to Series-I.

References:

[1] Pauluth D, Tarumi K, *J. Mater. Chem.*, 2004; 14 (8), 1219-1227.

[2] Pfletscher M, Hölscher S, Wölper C, Mezger M, Giese M, *Chem. Mater.*, 2017; 29 (19), 8462-8471.

[3] Sai D V, Zuhail K P, Sarkar R, Dhara S, *Liq. Cryst.*, 2015; 42 (3), 328-333.

[4] Walker R, *Liq. Cryst. Today*, 2020; 29(1), 2-14.

[5] Tadwee I, Shahi S, Ramteke V, Syed I, *Int. J. Pharm. Res. Allied Sci.*, 2012; (1), 6-11.

[6] Goodby J W, *Liq. Cryst.*, 2019; 46 (13– 14), 1901-1924.

[7] Demus D, *Mol. Cryst. Liq. Cryst.*, 1988; 165 (1), 45-84.

[8] Hird M, *Liq. Cryst. Today*, 2005; 14 (2), 9-21.

[9] Heppke G, Parghi D, Sawade H, *Liq. Cryst.*, 2000; 27 (3), 313-320.

[10] Shen D, Pegenau A, Diele S, Wirth I, Tschierske C, *J. Am. Chem. Soc.*, 2000; 122 (8), 1593-1601.

[11] Ali G Q, Tomi I H R. *Liq. Cryst.*, 2018; 45 (3), 421-430.

[12] Al-Obaidy M M A R, Tomi I H R, Jaffer H J, *Liq. Cryst.*, 2017; 44 (7), 1131-1145.

[13] Kirov N, Dozov I, Jordanova J, Hadjichristov G B, Fontana M P, *J. Mol. Struct.*, 2007; 839 (1-3), 84-89.

[14] Kohmoto S, Someya Y, Kishikawa K, *Liq. Cryst.*, 2010; 37 (2), 209-216.

[15] Murtaza G, Mumtaz A, Khan F A, Ahmad S, Azhar S, Khan S A, Najam Ui-Haq M, Atif M, Maalik A, *Acta. Pol. Pharm.*, 2014; 71 (4), 531-535.

[16] Qin W, Long S, Panunzio M, Biondi S, *Molecules*, 2013; 18 (10), 12264-12289.

[17] Fritsch L, Lavayen V, Merlo A A, *Liq. Cryst.*, 2018; 45 (12), 1802-1812.

[18] Gruzdev M S, Korolev V V, Ramazanova A G, Chervonova U V, Balmasova O V, *Liq. Cryst.*, 2018; 45 (6), 907-911.

[19] Paterson D A, Crawford C A, Pociecha D, Walker R, Storey J MD, Gorecka E, Imrie C T, *Liq. Cryst.*, 2018;45 (13-15), 2341-2351.

[20] Ge L-N, Xian S-W, Huang Y, Min Y, Lv J-M, Tian M, Yao D-S, *Liq. Cryst.*, 2018; 45 (7), 1055-1067.

[21] Ahmed HA, Mansour E, Hagar M, *Liq. Cryst.*, 2020; 47 (14-15), 2292-2304.

[22] Hagar M, Ahmed HA, Aouad MR, *Liq. Cryst.*, 2020; 47 (14-15), 2222-2233.
[23] Ahmed HA, Hagar M, Alhaddad OA, *Liq. Cryst.*, 2020; 47 (3), 404-413.
[24] Forsyth E, Paterson D A, Cruickshank E, Strachan G J, Gorecka E, Walker R, Storey J MD, Imrie C T, *J. Mol. Liq.*, 2020; 320, 114391.
[25] Walker R, Majewska M, Pociecha D, Makal A, Storey J MD, Gorecka E, Imrie C T, *ChemPhysChem.*, 2021; 22 (5), 461-470.
[26] Iftime M-M, Cozan V, Airinei A, Varganici C, Ailiesei G, Timpu D, Sava I, *Liq. Cryst.*, 2019; 46 (10), 1584-1594.
[27] Ahmed H A, Hagar M, El-Sayed T H, Alnoman R B, *Liq. Cryst.*, 2019; 46 (7), 1156-1166.
[28] Abberley J P, Killah R, Walker R, Storey J MD, Imrie C T, Salamończyk M, Chenhui Z, Gorecka E, Pociecha D, *Nat. Commun.*, 2018; 9, 228.
[29] Salamończyk M, Vaupotič N, Pociecha D, Walker R, Storey J MD, Imrie C T, Wang C, Zhu C, Gorecka E, *Nat. Commun.*, 2019; 10, 1922.
[30] Ahmed HA, Hagar M, Saad G, *Liq. Cryst.*, 2019; 46 (11), 1611-1620.
[31] Abberley J P, Walker R, Storey J MD, Imrie C T, *Liq. Cryst.*, 2020; 47 (8), 1232-1245.
[32] Dave J, Bhatt H, *Mol. Cryst. Liq. Cryst.*, 2012; 562, 1-9.
[33] Jain B, Patel R, *Mol. Cryst. Liq. Cryst.*, 2016; 637, 1-9.
[34] Ahmed N, Saad G, Naoum M, *Liq. Cryst.*, 2019; 46, 1631-1642.
[35] Prajapati A, Varia M, *Liq. Cryst.*, 2008; 35, 1271-1277.
[36] Gray G W, *London, UK: Academic Press;* 1979; p. 285 316.
[37] Goodby J W, *Liq Cryst.*, 2019; 46, 1901-1924.
[38] Matsui M, Kamino Y, Hayashi M, Funabiki K, Shibata K, Muramatsu H, Kaneko M, *Liquid Crystals*, 1998; 25(2), 235-240.
[39] Gray G W, Jones B, *J Chemical Society*, 1954; 678-683.
[40] Gray G W, Jones B, *J Chemical Society*, 1954; 2556-2562.
[41] Gray G W, Jones B, *J Chemical Society*, 1955
[42] Jones B, *J Chemical Society*, 1935; 1874.
[43] Dave J S, Vora R A, *Liquid Crystals and Ordered Fluids* (eds),1970; Johnson J F, Porter R S, *Newyork: Plenum*, 477.